Supporting information for

Enhancing oxide-ionic conductivity of $Ba_3Mo_{1+x}Nb_{1-2x}Ge_xO_{8.5}$ at intermediate temperatures: the effect of site-selective Ge^{4+}-substitution

Zien Cheng,[a] Jia Yang,[b] Pengfei Jiang,[a,*] He Huang,[a] Ivan da-Silva,[c] Wenliang Gao,[a] Rihong Cong,[a] Tao Yang[a,*]

[a] College of Chemistry and Chemical Engineering, Chongqing University, Chongqing 401331, P. R. China

[b] School of Chemistry and Chemical Engineering, Yangtze Normal University, Chongqing 408100, P. R. China

[c] ISIS Facility, Rutherford Appleton Laboratory, Chilton, Didcot, OX110QX, United Kingdom

* E-mail: pengfeijiang@cqu.edu.cn, taoyang@cqu.edu.cn.

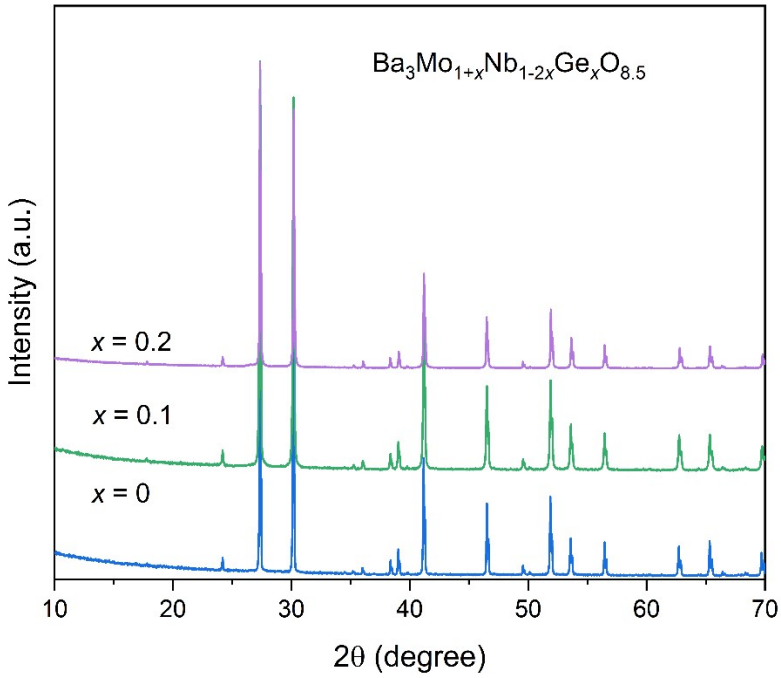

Figure S1. Powder X-ray diffraction patterns of $Ba_3Mo_{1+x}Nb_{1-2x}Ge_xO_{8.5}$ ($x \leq 0.2$)

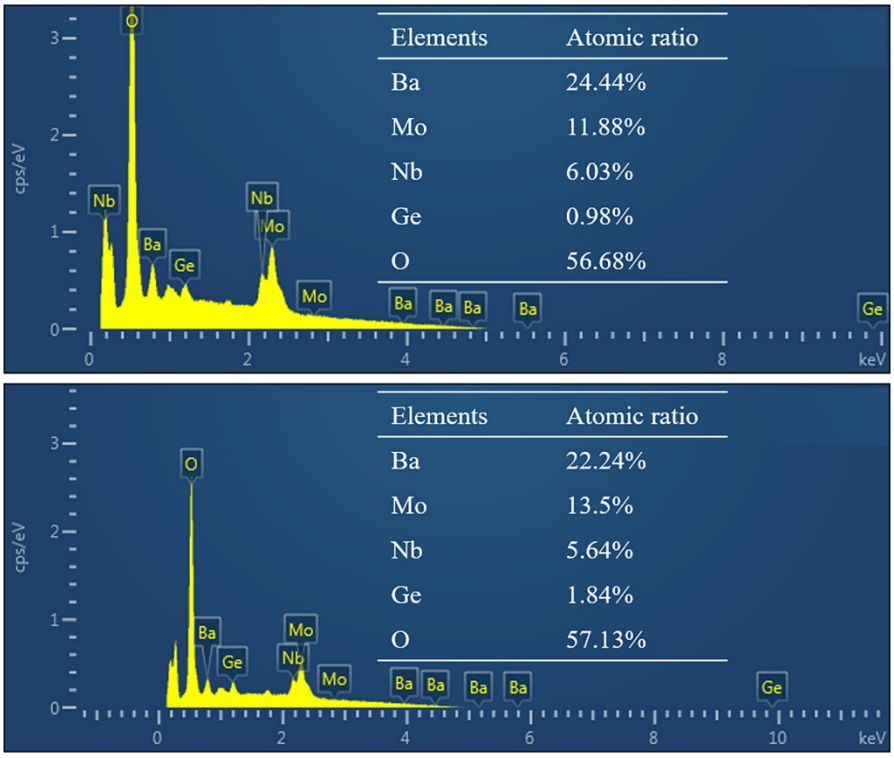

Figure S2. The Energy Dispersive X-ray (EDX) spectra for $Ba_3Mo_{1.2}Nb_{0.6}Ge_{0.2}O_{8.5}$ recorded on two particles. The insets show the detected atomic ratios.

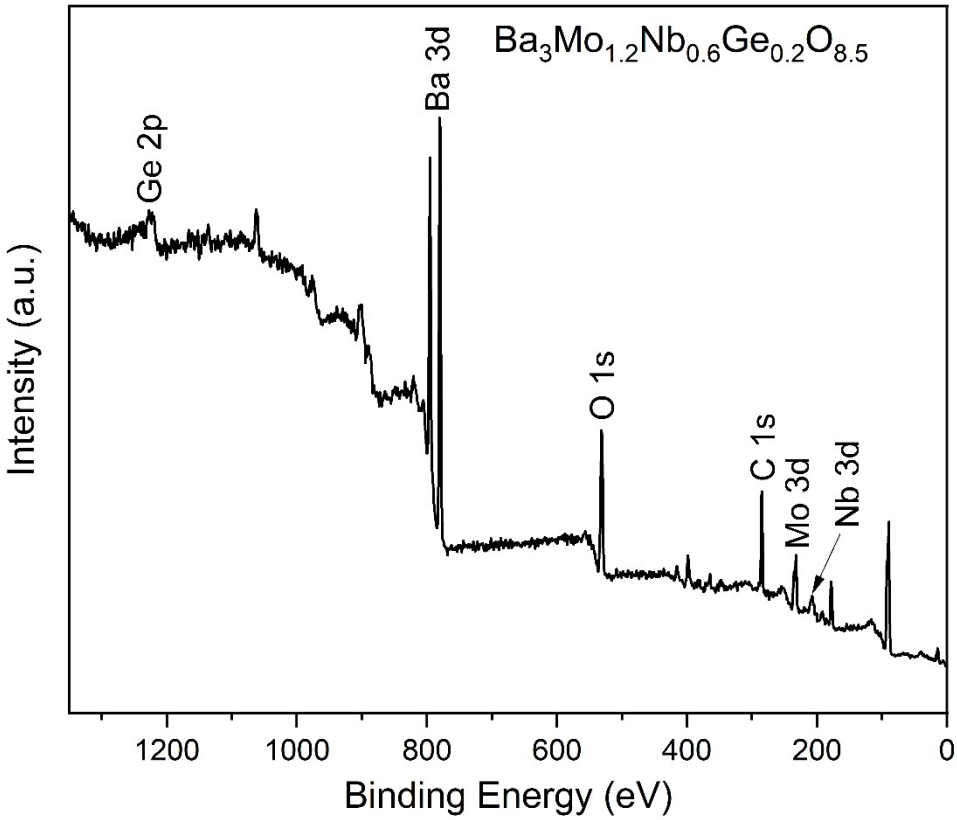

Figure S3. The survey XPS of $Ba_3Mo_{1.2}Nb_{0.6}Ge_{0.2}O_{8.5}$.

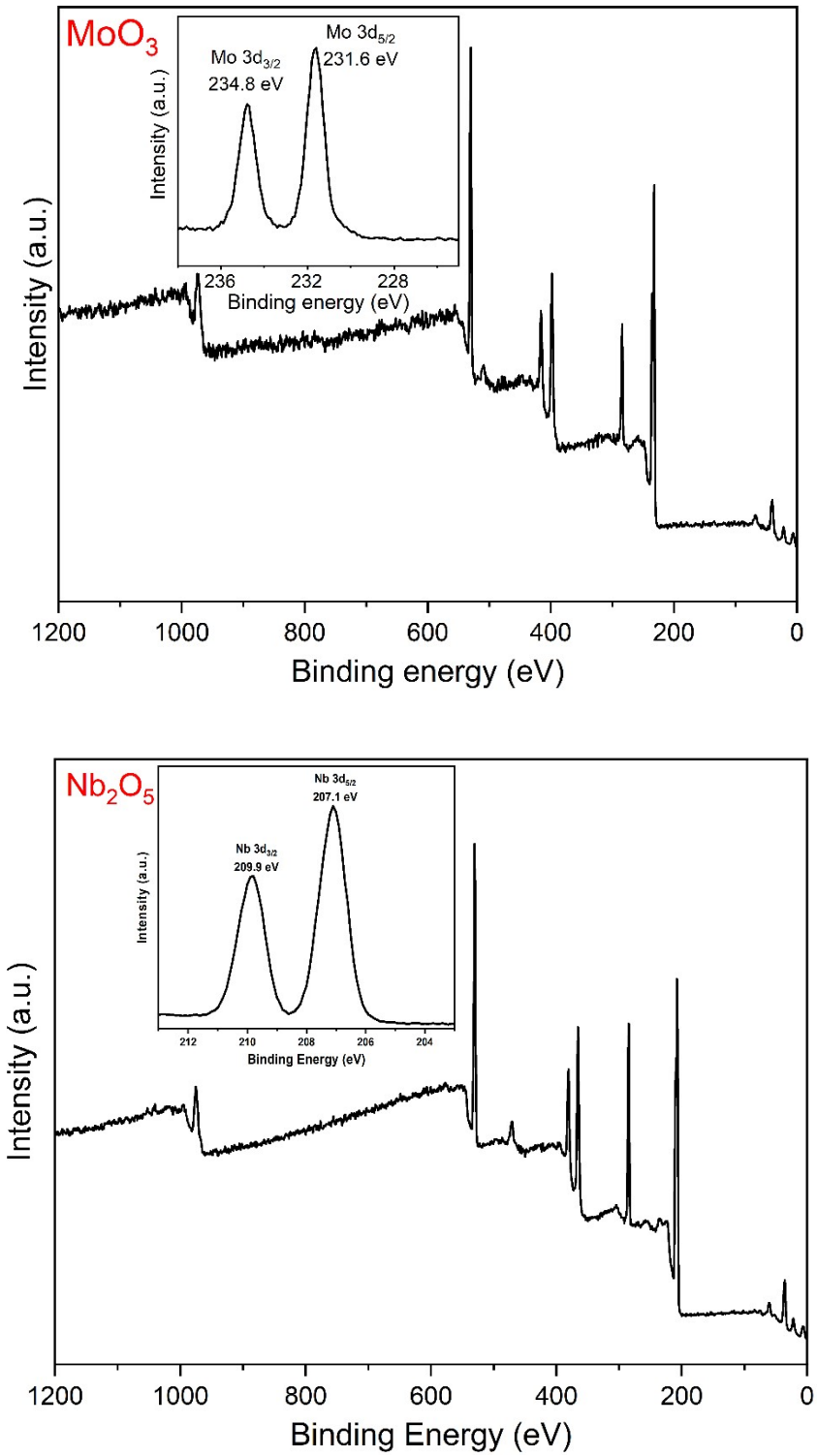

Figure S4. The survey XPS of MoO_3 and Nb_2O_5. The inset shows the Mo 3d and Nd 3d signals.

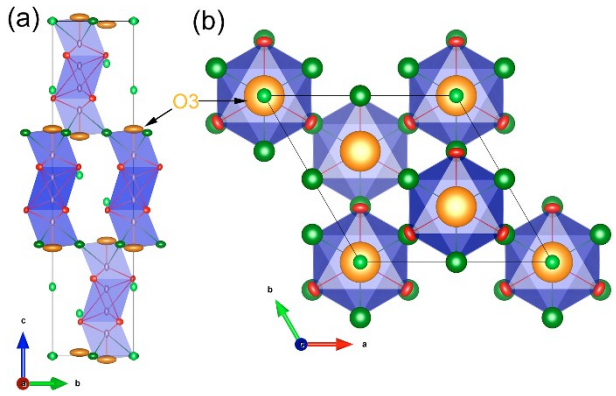

Figure S5. Crystal structure of $Ba_3Mo_{1.2}Nb_{0.6}Ge_{0.2}O_{8.5}$ with atomic displacement ellipsoids drawn at 50% probability.

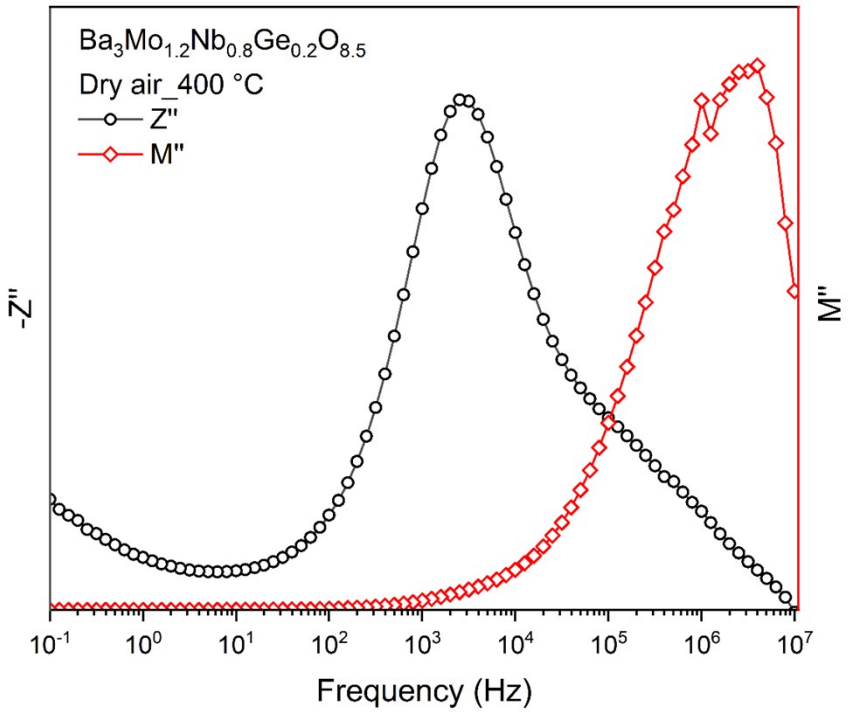

Figure S6. Plots of the imaginary part of the impedance (Z") and electrical modular (M") along with frequency.

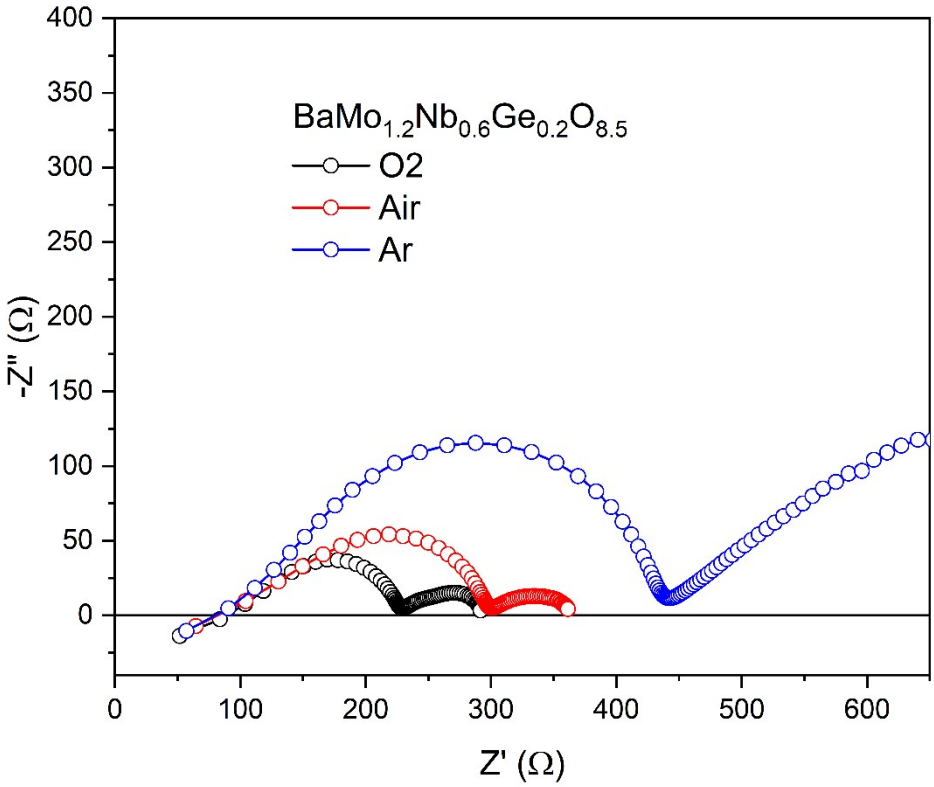

Figure S7. Complex impedance plots of $Ba_3Mo_{1.2}Nb_{0.6}Ge_{0.2}O_{8.5}$ recorded in dry air, O2, and Ar atmospheres at 550 ºC.

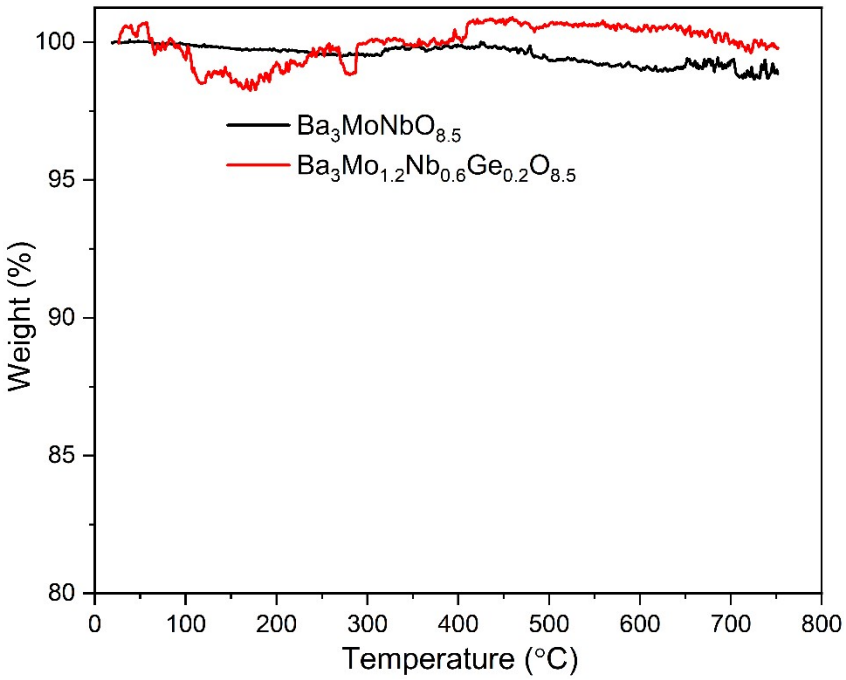

Figure S8. TGA curves for $Ba_3Mo_{1+x}Nb_{1-2x}Ge_xO_{8.5}$ with x = 0 and 0.2 measured under air atmospheres.

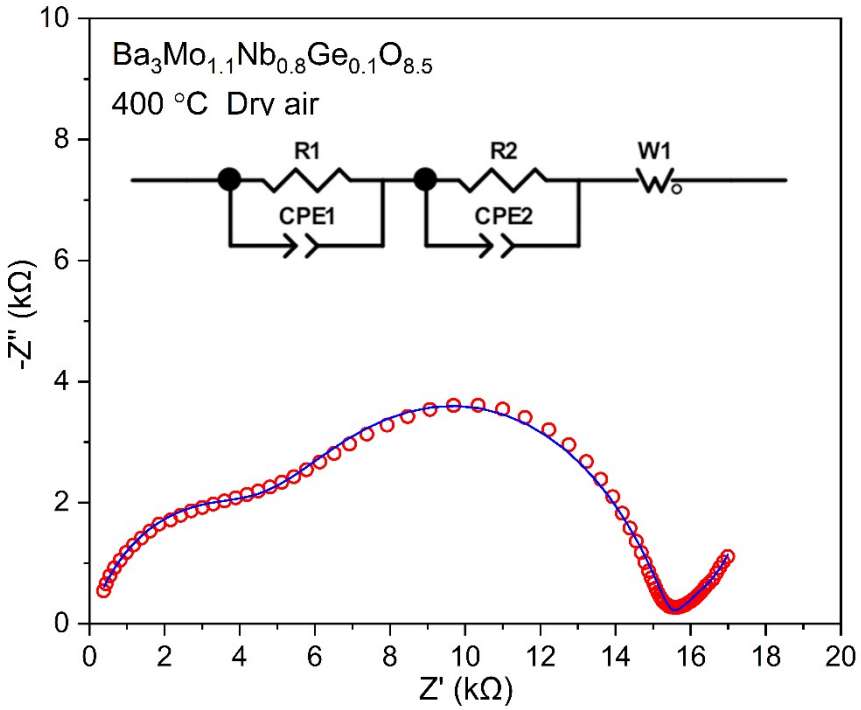

Figure S9. An impedance spectrum fit for $Ba_3Mo_{1.1}Nb_{0.8}Ge_{0.1}O_{8.5}$. The inset shows the equivalent circuit, where R, CPE, and W represent the resistor, constant phase element, and electrode response.

Table S1. The atomic coordinates, occupancies, anisotropic thermal displacement parameters, bond valence sums for $Ba_3Mo_{1.4}Nb_{0.6}Ge_{0.2}O_{8.5}$ obtained from Rietveld refinement against neutron powder diffraction data.[a]

Site	Ba1	Ba2	Mo1/Nb1/Ge1	Mo2/Nb2	O1	O2	O3
x	0	0	0	0	0.17196(2)	0	0.0836(4)
y	0	0	0	0	0.34392(2)	0.5	0.0097(8)
z	0	0.2063(1)	0.40052(5)	0.4716(9)	0.1025(5)	0	0.3231(2)
BVS	2.06	2.00	5.54/5.00/3.60	4.33/4.16	-1.97	-1.39	-2.23
Occ.	1	1	0.5773(8) 0.2877(4) 0.1	0.0247(8) 0.0123(4)	1	0.408(2)	0.1063(6)
U_{11} (Å^2)	0.0232(2)	0.0232(2)	0.0140(2)	0.0094(4)	0.0249(6)	0.0468(2)	0.033(2)
U_{22} (Å^2)	0.0232(2)	0.0232(2)	0.0140(2)	0.0094(4)	0.0138(1)	0.0468(2)	
U_{33} (Å^2)	0.0306(7)	0.0306(7)	0.0314(9)	0.0273(7)	0.0186(9)	0.013(3)	
U_{12} (Å^2)	0.0116(3)	0.0116(3)	0.0070(3)	0.0047(2)	0.0069(6)	0.0234(9)	
U_{13} (Å^2)	0	0	0	0	0.0021(3)	0	
U_{23} (Å^2)	0	0	0	0	0.0010(2)	0	

[a]The thermal factor of O3 was refined with a single *U* factor; For for O2 and the cations, $U_{11} = U_{22} = 2U_{12}$, $U_{13} = U_{23} = 0$; For O1, $U_{22} = 2U_{12}$, $U_{23} = 2U_{13}$.

Table S2. Selected interatomic distances in $Ba_3Mo_{1.4}Nb_{0.6}Ge_{0.2}O_{8.5}$.

Bond	Length (Å)	Bond	Length (Å)
M1/Ge-O3	1.699(4)	Ba1-O1 × 6	2.7902(8)
M1/Ge-O1 × 3	1.8143(8)	Ba1-O2 × 6	2.9556(4)
M1/Ge-O2 × 3	2.2189(9)	Ba2-O3	2.520(4)
M2-O1× 3	1.805(8)	Ba2-O1 × 3	2.801(2)
M2-O1× 3	2.58(2)	Ba2-O1 × 6	3.0036(4)